journal of the mechanical behavior of biomedical materials 140 (2023) 105729

Contents lists available at ScienceDirect

Journal of the Mechanical Behavior of Biomedical Materials

journal homepage: www.elsevier.com/locate/jmbbm

The Spider Silk Standardization Initiative (S3I): A powerful tool to harness biological variability and to systematize the characterization of major ampullate silk fibers spun by spiders from suburban Sydney, Australia

Sean Blamires [a,b,c], Paloma Lozano-Picazo [d,e], Augusto Luis Bruno [d,e], Miquel Arnedo [f], Yolanda Ruiz-León [g], Daniel González-Nieto [d,h,i], Francisco Javier Rojo [d,e,j], Manuel Elices [e], Gustavo Víctor Guinea [d,e,i,j], José Pérez-Rigueiro [d,e,i,j,*]

[a] Evolution and Ecology Research Centre, University of New South Wales, Sydney, NSW, 2052, Australia
[b] NMR Facility, Mark Wainwright Analytical Centre, University of New South Wales, Sydney, NSW, 2052, Australia
[c] School of Mechanical and Mechatronic Engineering, University of Technology, Sydney, NSW, 2007, Australia
[d] Centro de Tecnología Biomédica, Universidad Politécnica de Madrid, 28223, Pozuelo de Alarcón, Madrid, Spain
[e] Departamento de Ciencia de Materiales, ETSI Caminos, Canales y Puertos, Universidad Politécnica de Madrid, 28040, Madrid, Spain
[f] Department de Biologia Evolutiva, Ecologia i Ciencies Ambientals, and Biodiversity Research Institute (IRBio), Universitat de Barcelona, 08028, Barcelona, Spain
[g] Research Support Unit, Real Jardín Botánico, Consejo Superior de Investigaciones Científicas (CSIC), 28014, Madrid, Spain
[h] Departamento de Tecnología Fotónica y Bioingeniería, ETSI Telecomunicaciones, Universidad Politécnica de Madrid, 28040, Madrid, Spain
[i] Centro de Investigación Biomédica en Red de Bioingeniería, Biomateriales y Nanomedicina (CIBER-BBN), Instituto de Salud Carlos III, Spain
[j] Grupo de Biomateriales y Medicina Regenerativa, Instituto de Investigación Sanitaria del Hospital Clínico San Carlos (IdISSC), Calle Prof. Martín Lagos s/n, 28040, Madrid, Spain

ARTICLE INFO

Keywords:
Spider silk
Tensile properties
Variability
Supercontraction
α* parameter
Spider silk standardization initiative

ABSTRACT

The true stress-true strain curves of 11 Australian spider species from the Entelegynae lineage were tensile tested and classified based on the values of the alignment parameter, α*, in the framework of the Spider Silk Standardization Initiative (S3I). The application of the S3I methodology allowed the determination of the alignment parameter in all cases, and were found to range between $\alpha^* = 0.03$ and $\alpha^* = 0.65$. These data, in combination with previous results on other species included in the Initiative, were exploited to illustrate the potential of this approach by testing two simple hypotheses on the distribution of the alignment parameter throughout the lineage: (1) whether a uniform distribution may be compatible with the values obtained from the studied species, and (2) whether any trend may be established between the distribution of the α* parameter and phylogeny. In this regard, the lowest values of the α* parameter are found in some representatives of the Araneidae group, and larger values seem to be found as the evolutionary distance from this group increases. However, a significant number of outliers to this apparent general trend in terms of the values of the α* parameter are described.

1. Introduction

Spider silk is a unique material, tougher than Kevlar and stronger than steel. Therefore, there is great interest in harnessing its properties within synthetically spun fibers. Thus, understanding how and why spiders have evolved to spin silks with such impressive properties is of paramount importance (Anton et al., 2017; Blackledge, T. A. et al., 2009; Blackledge et al., 2012; Blamires, S., 2022; Heim et al., 2009; Perez-Rigueiro et al., 2021).

Another reason why researchers are interested in performing comparative analyses of silk properties is because spider silks and webs represent an extended phenotype, which may evolve differently and/or independently to regular phenotypes since they may, in certain instances, engineer ecosystems (Hansell, 2007). They nevertheless may exhibit phenotypic plasticity in a similar way to regular phenotypes (Blamires, 2010; Blamires et al., 2017a); that is, their structure and property can vary substantially across species and ecological contexts (Blackledge, T. A. and Hayashi, 2006; Blamires et al., 2017b; Blamires et al., 2017a; Boutry and Blackledge, 2010).

The diversification in types and properties of spider silk has come

* Corresponding author. Centro de Tecnología Biomédica, Universidad Politécnica de Madrid, 28223, Pozuelo de Alarcón, Madrid, Spain.
E-mail address: jose.perez@ctb.upm.es (J. Pérez-Rigueiro).

https://doi.org/10.1016/j.jmbbm.2023.105729
Received 7 November 2022; Received in revised form 23 January 2023; Accepted 11 February 2023
Available online 13 February 2023

about over almost 400 million years of evolution (Anonymous, 2019; Selden et al., 2008), and may be identified at various levels, including the genomic, transcriptomic, and proteomic (Aparecido dos Santos-Pinto et al., 2018; Aparecido dos Santos-Pinto et al., 2019), as well as in the evolved glandular organization (Blackledge, T. A. and Hayashi, 2006; Vollrath, 1994). As a result, a broad set of specialized silk fibers has become adapted to fulfil many specific requirements for the more than 40000 extant spider species (Anonymous, 2019). The fibers spun from the major ampullate glands (MAS), in particular, are responsible for such critical functions as constituting the lifeline that the spider uses to escape from predators, and building the structural parts of the webs (Blackledge, T. A. et al., 2009; Swanson et al., 2006). It was initially assumed (Rudall and Kenchington, 1971) that the evolution of MAS along the phylogeny of the web building spiders, in combination with the various ecological niches occupied by the different spider species, would result in an extremely wide range of microstructures (Asakura et al., 2018; Riekel et al., 1999) and properties (Blackledge et al., 2012) in the fibers. However, the lack of reproducibility that has been found when characterizing the mechanical behaviour of spider silk, even if spun by a single specimen (Dunaway et al., 1995; Madsen et al., 1999), was found to be a major drawback for any attempt intended to determine and systematize the whole extension of properties exhibited by MA silks.

In this context, the definition of the α* parameter (Madurga et al., 2016) and its application in the framework of the Spider Silk Standardization Initiative (S3I) (Garrote et al., 2020) constitute a systematic methodology to classify the whole range of tensile properties measured from the MAS fibers of Entelegynae species within a common one-dimensional parametric space. As explained below, and summarized in the Appendix, the α* parameter is an experimental magnitude that is calculated through the comparison of the true stress-true strain curve of the MAS fiber of interest with a reference true stress-true strain curve, determined from the MAS fibers spun by the spider *Argiope aurantia*.

In order to remove the variability found in MA silk, even if retrieved from a single web (Perez-Riguero et al., 2001), the measurement of the α* parameter relies on the uniformization induced by maximum supercontraction on the properties exhibited by these fibers. Supercontraction is a phenomenon characteristic of MA silk that was first identified by the significant reduction in length when the fiber is immersed in water (Work, 1977). Although it was initially considered little more than a curiosity, it was later acknowledged that supercontraction reflects some profound design principles of the material and, in particular, the contribution of the elastomeric behaviour of the protein chains to the mechanical behaviour of the material (Gosline et al., 1984). From a practical point of view, it is found that supercontraction may be exploited to tailor the tensile properties of MAS fibers (Perez-Rigueiro, J. et al., 2003), so that it opens the possibility of establishing precise quantitative comparisons between different samples. In particular, the application of maximum supercontraction allows defining a ground state of MA silk that can be reached repeatedly and independently from the previous loading history of the material (Elices et al., 2004; Perez-Rigueiro, J. et al., 2003).

Following this rationale, it was possible to obtain a first qualitative classification of the properties exhibited by MAS fibers (Blackledge et al., 2012) spun by different species by comparing the stress-strain curves of MA silks after being subjected to maximum supercontraction. This initial study showed that distantly related species, such as *Argiope lobata* and *Nephila inaurata* do spin fibers indistinguishable from the point of view of their mechanical behaviour, while these properties differ from those measured in other representatives of the *Argiope* genus.

Based on these ideas, it was found that it is possible to assign to each stress-strain curve obtained from MAS fibers a single parameter, α* (alpha-star) (Madurga et al., 2016), that allows the classification of the material spun by each species of interest using a one-dimensional parametric space. The determination of the α* parameter, requires following a simple procedure that implies: (1) Tensile testing MAS fibers of any given species after being subjected to maximum supercontration, (2) calculating the true stress-true strain curve (see below for the details of this calculation), and (3) comparing the true stress-true strain curve of interest with a Reference true stress-true strain curve that was obtained from the MAS of the species *Argiope aurantia*. The comparison between the curve of interest and the Reference curve proceeds by displacing the true stress-true strain curve of interest along the X-axis (true strain axis) until both curves concur at high values of true strain. The α* parameter simply measures the displacement along the X-axis required to get an adequate concurrence between both curves. The procedure for calculating the α* parameter is summarized step by step in the Appendix.

The possibility of classifying the behaviour of the MAS fibers using the α* parameter led to the launching of the Spider Silk Standardization Innitiative (S3I) as an effort to compile the values of the α* parameter from as many spider species and geographical locations as possible (Garrote et al., 2020). Following the usual procedure, the MAS fibers of a set of representative spider species sampled from a well-defined geographical location, in this case a single urban location in Sydney (Australia), were accordingly herein characterized.

Since silk variability due to phylogeny, genetics, chemistry, and ecology can obscure our interpretations about how silk plasticity evolved and its functional value, the availability of a large number of α* parameters constitutes a tool that can allow the application of Big Data analysis/data mining and Artificial Intelligence (AI)/machine learning methodologies to find solutions to such seemingly difficult questions to answer. In this context, this work represents a contribution to the effort intended to obtain an overall description of the genome, microstructure and mechanical properties of spider silk (Arakawa et al., 2022), and not only expands the set of α* parameters available in S3I to new spider species, but also offers a first detailed illustration of the type of analyses that may be undertaken in the framework of this initiative.

2. Materials and methods

2.1. Spider handling, housing and silking procedures

All 11 species of spiders used herein were collected on or near the Kensington Campus of the University of New South Wales in Sydney, Australia, during the summer (December through February) on 2020–2021. *Trichonephila plumipes*, *Badumna longinqua*, *Leucauge dromadaria*, *Argiope keyserlingi*, *Plebs ebernus*, and *Phongnatha graefei* were collected during the day (09:00–19:00 h), while *Eriophora transmarina*, *Dienopis subrufa*, *Latrodectus hasselti*, *Steatoda grossa*, and *Neosparassa diana* were collected at night (i.e. 20:00–24:00 h). A minimum of two specimens and maximum of 12 specimens (*T. plumipes*, *B. longinqua, L. hasselti*, *A. keyserlingi*, *D. subrufa*) were collected for any of the species. Upon collection the spiders were returned to the Spider Silk Research Lab at the University of New South Wales and housed as follows.

T. plumipes and *E. transmarina* were housed in 700 mm (high) x 700 mm (wide) x 120 mm (deep) Perspex frames with front and back Perspex lids. Meanwhile, *B. longinqua*, *A. keyserlingi*, *P. ebernus*, and *P. graefei* were housed in 300 mm (high) x 300 mm (wide) x 80 mm (deep) Perspex frames with front and back Perspex lids. *L. dromadaria*, and *L. hasselti* were housed in 220 mm (high) x 270 mm (wide) x 180 mm (deep) aquaria, while *S. grossa* and *N. diana* were housed in 170 mm (high) x 210 mm (wide) x 130 mm (deep) aquaria. *D. subrufa* were kept in upturned 500 ml plastic cups. Additional wooden and/or cardboard materials were included into the aquaria or cups to provide a framework for the spiders to build their webs.

All spiders were kept at ~21 °C and ~60% RH for a maximum of three weeks and fed crickets once per week. Water was supplied by spraying water onto tissue lining the base of the enclosures/aquaria, or by adding moist cotton wool to the enclosure (in the case of *D. subrufa*).

We anaesthetized each spider collected using CO_2 and pinned them

to a Styrofoam board before carefully pulling a single MA silk fiber from their spinnerets using tweezers. The silk threads were mounted onto individual 10 mm × 10 mm cardboard frames following procedures outlined by Benamu et al. (2017) (Benamu et al., 2017), Blamires et al. (2018) (Blamires et al., 2018), and Viera et al. (2019) (Viera et al., 2019). We weighed the spiders immediately upon collection and prior to silking to ensure that capture and/or housing the spiders did not result in significant (>20% of captured body mass) weight loss.

2.2. Mechanical characterization

Silk fibers were transferred from the cardboard frames used for their retrieval to plastic foil frames and fixed at their ends with ethyl-cyanoacrylate, as described elsewhere (Perez-Rigueiro, J. et al., 1998). The distance between both fixed ends was measured with a calliper. A small length of the original sample was preserved for the measurement of the cross sectional area, as described below.

The process of maximum supercontraction of the fibers proceeded as described elsewhere (Perez-Rigueiro, J. et al., 2003). Briefly, the plastic foil frame was fixed to the tensile testing machine (Instron 4411) and the edges were cut. The upper crosshead was displaced until the zero load condition was reached (i.e. the fiber is not subjected to load but taut) and the initial length before supercontraction, L_0, was calculated from the initial length measured with a calliper, corrected with the displacement of the crosshead. In order to reach maximum supercontraction, the upper crosshead was displaced to reduce the distance between both fixed ends of the fiber, immersed in water and allowed to dry overnight before being tensile tested.

The tensile test started with the verification that the fiber was not loaded after supercontraction (otherwise the fiber would be subjected to controlled, but not maximum supercontraction (Perez-Rigueiro, J. et al., 2003)). The length of the fiber after maximum supercontraction, L_{MS}, was calculated from the initial length, L_0, after substracting the distance that the fiber was allowed to supercontract and corrected by the displacement of the crosshead required to determine the zero load condition of the maximum supercontracted sample.

Tensile tests on the maximum supercontracted fibers were performed in a 4411 Instron tensile testing machine with the lower grip supported on a precision balance (Precisa XT220A, maximum load 200 gf, resolution 0.1 mgf). Tensile tests were performed at a constant speed of 1 mm/min in air (nominal environmental conditions 25 °C, 35% relative humidity) and the displacement of the crosshead was taken directly as a measurement of the displacement of the fiber (Perez-Rigueiro, J. et al., 1998).

The cross-sectional areas of the MAS fibers were calculated from scanning electron (SEM) micrographs of the fragments preserved before proceeding with the tensile testing under the assumption of a circular cross section (Perez-Riguero et al., 2001). Fibers were coated with gold in a sputter coated (Q150R S plus Quorum) and micrographs were obtained in a Hitachi S-3000-N SEM at 10 kV. The cross sectional area of the maximum supercontracted samples, A_{MS}, was calculated from the area determined prior to supercontraction, A_0, under the hypothesis that the volume of the fiber remains constant during supercontraction (Guinea et al., 2006) as:

$$A_0 L_0 = A_{MS} L_{MS} \tag{1}$$

Engineering strain, e, and stress, s, were calculated from the length, L_{MS}, and from the cross sectional area, A_{MS}, after supercontraction as:

$$e = \frac{\Delta L}{L_{MS}} \quad ; \quad s = \frac{F}{A_{MS}} \tag{2}$$

True strains, ε, and true stresses, σ, were calculated from the engineering magnitudes, again assuming a constant volume (Guinea et al., 2006) as:

$$\varepsilon = Ln(1+e) \quad ; \quad \sigma = s(1+e) \tag{3}$$

3. Results and discussion

Representative true stress-true strain curves of MAS fibers from each species included in this study are compared in Fig. 1 with the *Argiope aurantia* reference to illustrate the procedure employed for calculating the α* parameter. The species of the genus Araneidae, Desidae and Deinopidae are shown in Fig. 1a, while those of the genus Theriidae, Tetragnatidae, Sparassidae and Nephilinae are presented in Fig. 1b. The

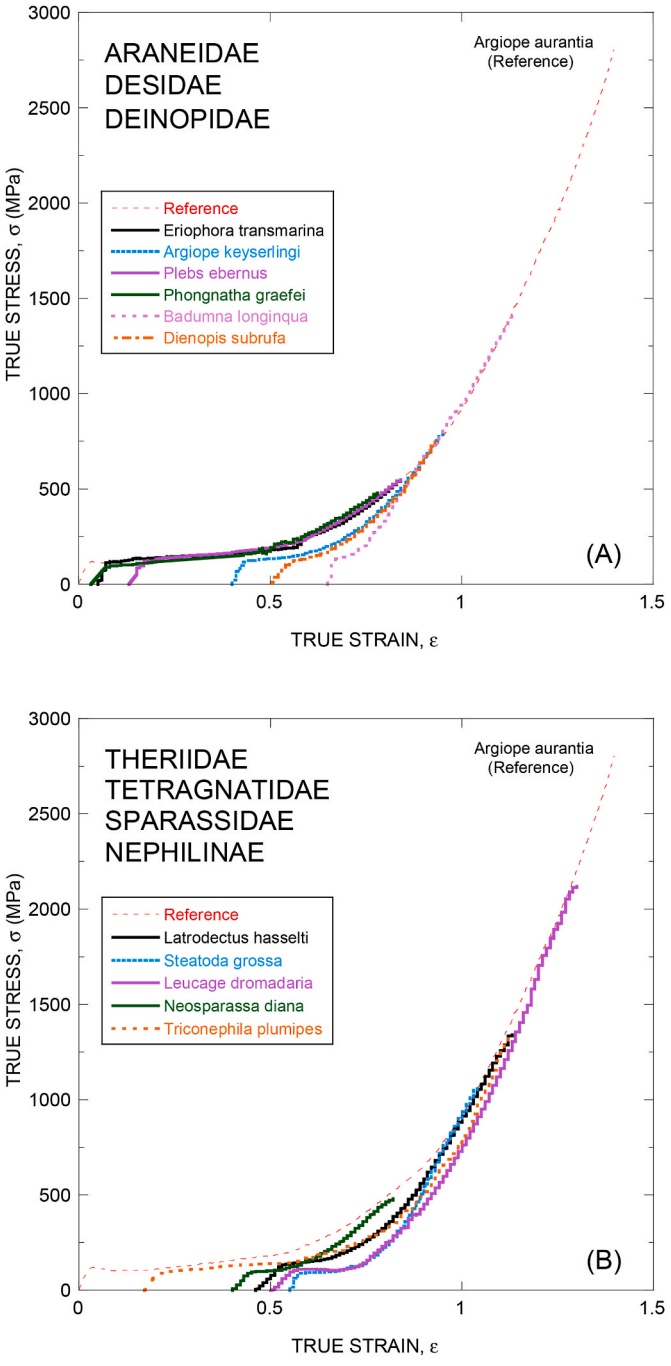

Fig. 1. Representative true stress-true strain curves of the MA silk fibers retrieved from the different species used for the calculation of the α* parameter. (A) Araneidae (*Eriophora transmarina*, *Argiope keyserlingi*, *Plebs ebernus*, and *Phongnatha graefei*), Desidae (*Badumna longinqua*) and Deinopidae (*Dienopis subrufa*). (B) Theriidae (*Latrodectus hasselti* and *Steatoda grossa*), Tetragnatidae (*Leucage dromadaria*), Sparassidae (*Neosparassa diana*), and Nephilinae (*Triconephila plumipes*).

records of all species may be retrieved from the webpage of the Spider Silk Standardization Initiative at www.ctb.upm.es/core-facilities/.

In all cases the concurrence of each true stress-true strain curve with the *A. aurantia* reference curve at high strains is apparent. As explained above, the quantitative value of the α* parameter is calculated by displacing the true stress-true strain curve of interest along the true strain axis until two conditions, as established in Garrote et al., (2020) (Garrote et al., 2020), are fulfilled: (1) The value of the true stresses of the (displaced along the X axis) curve under study and that of the reference must concur at a given value of true strain, and (2) the slopes of both curves at the point of concurrence must not differ by more than 20%. This two conditions may be implemented manually as detailed in the Appendix or using the Macro Alpha MA Silk Calculator v2, that can be downloaded from www.ctb.upm.es/core-facilities/.

Three or four samples were tensile tested for each species, except for *T. plumipes* from which only two samples were retrieved. The value of the α* parameter was calculated from each individual curve and the value assigned to a species was determined as the arithmetic mean of the values obtained from the individual curves. In all cases, the standard error of the α* for a given species was found to be equal or lower than 0.05, as established in a previous work. The values of the α* parameters are summarized in Table 1.

The definition of the α* parameter allows quantifying the differences found in the MAS fibers spun by different Entelegynae spider species and, consequently, it may be used to correlate these differences with various aspects of the ecology and phylogeny of the different species. In turn, these correlations represent a valuable guide to understand the molecular mechanisms that underpin the variations observed in the tensile properties of the fibers and on the evolutionary pressures that modelled them in the past. Evidently, the fulfilment of this program implies the determination of a significant number of α* parameters obtained from an ample set of species and geographical locations. In this regard, the limited number of available α* parameters at the time of the writing (i.e. seven Peruvian spiders (Garrote et al., 2020) and the eleven species included in the present study) only allows a modest approach to the ambitious comprehensive objective. However, even with these limited set of data it is possible to establish some promising trends that illustrate the potential of this methodology.

3.1. Overall distribution of the α* parameter

The overall distribution of the α* parameters obtained by combining the results previously determined from a set a Peruvian spiders (Garrote et al., 2020) and those calculated in this work are shown in Fig. 2.

Although the number of available data is, at present, too limited to establish any definitive conclusion with respect to the exact distribution of the α* values, it is remarkable how there seems to be a relatively uniform distribution of these values among all the studied species. In other words, it seems to be possible to find at least one example for each value of the α* parameter, even when the small number of characterized species is considered. Consequently, it is reasonable to test the hypothesis of whether the overall distribution of the α* may correspond to a uniform distribution, i.e. if the probability of obtaining a value of the α* parameter from any species chosen at random and with no consideration of its phylogeny or ecology, is essentially a constant. The χ^2 Test of Goodness of Fit may be used to check this hypothesis, as described below.

Table 1
Summary of the values of the α* parameter for all the spider species included in this study.

Family	Species	α*
Araneidae	*Eriophora transmarina*	0.05 ± 0.01
Araneidae	*Plebs ebernus*	0.13 ± 0.04
Araneidae	*Phongnatha graefei*	0.03 ± 0.02
Araneidae	*Argiope keyserlingi*	0.38 ± 0.05
Nephilinae	*Triconephila plumipes*	0.18 ± 0.03
Theriidae	*Steatoda grossa*	0.52 ± 0.04
Theriidae	*Latrodectus hasselti*	0.48 ± 0.04
Sparassidae	*Neosparassa diana*	0.42 ± 0.02
Deinopidae	*Dienopis subrufa*	0.44 ± 0.05
Desidae	*Badumna longinqua*	0.65 ± 0.01
Tetragnathidae	*Leucage dromadaria*	0.44 ± 0.04

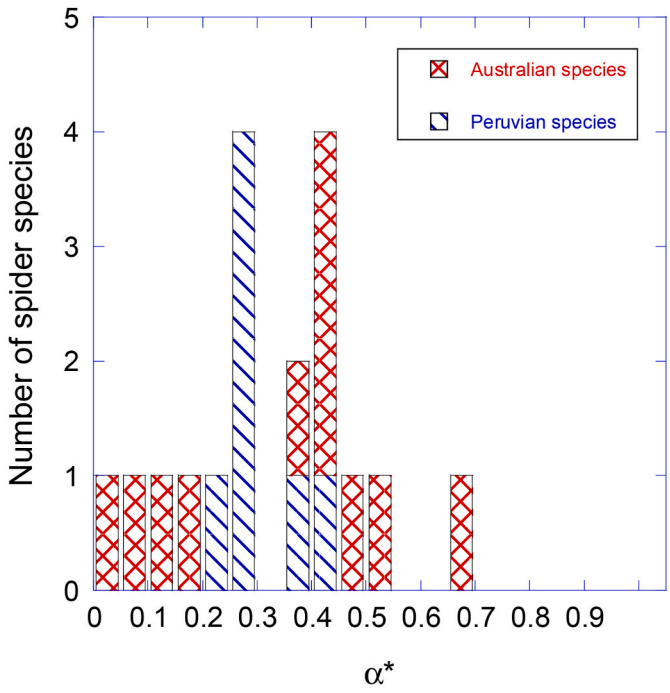

Fig. 2. Overall distribution of the α* parameter among a set of peruvian (Garrote et al., 2020) and australian (data presented in this work) spider species included in S3I.

The application of the Test of Goodness of Fit to any statistical variable requires defining a set of equal intervals that comprise all the possible values that the statistical variable may take. In this case, and considering that the precision of the α* parameter for a given species is estimated as 0.05, this will be the value used for defining the intervals (i.e. from 0 to 0.05, from 0.05 to 0.1, etc.). The determination of a uniform distribution requires establishing the maximum value accessible to the variable, since this maximum value (in combination with the width of each interval) defines the number of intervals to be considered. In this case, the maximum value of α* found in the Australian spiders corresponds to α* = 0.65 (*B. longinqua*) and it is larger than the maximum value found in the Peruvian specimens. However, the largest value found for the α* parameter in any of the characterized species at the moment of writing this work was determined for the spider *Phidippus regius* (Madurga et al., 2016) with α* = 0.82. Consequently, the null hypothesis will correspond to a uniform distribution of the α* parameter between the values α* = 0.0 and α* = 0.85 and the analysis will employ intervals with a value Δα* = 0.05. The corresponding value of the X^2 test may be calculated to be $X^2 = 26.0$ which is to be compared with the value of the χ^2 function for f = 17 degrees of freedom (the degrees of freedom corresponds to the number of intervals minus 1) for a level of significance of 5%, $\chi^2_{5\%}$ (f = 17) = 27.59. Since $X^2 < \chi^2$ the null hypothesis cannot be rejected for this level of significance, which supports that the data on the overall distribution of the α* parameters are compatible with a uniform function between the values α* = 0.0 and α* = 0.85. As indicated above, this calculation must only be considered as reflecting a trend to an approximate uniform covering of the α* values within these limits when no other condition is used to classify the spider species. It is to be expected that some preferred intervals will be found

when the analysis is refined to include, for instance, phylogeny.

3.2. Phylogenetic distribution of the α* parameter

The distribution of the values of the α* parameter across the phylogeny in the characterized species is presented in Fig. 3. As expected from the previous discussion, the values of the α* parameter cover the whole range between α* = 0.0 and α* = 0.65 continuously without any apparent gap or range of missing values.

The consideration of the phylogenetic relationship among the various species, however, allows proposing some preliminary trends. Thus, the lowest values of the α* parameter are consistently found in the Araneidae family, and it may be argued that there is a tendency to observe higher values of the α* parameter with increasing evolutionary distance from this group. There are, however, significant outliers to this apparent general trend. Thus, the largest values of α* parameter within the Araneoidea are found in the genus *Argiope* (*A. argentata* and *A. keyserlingi*), even despite the MAS of the *Argiope aurantia* species is used to define the Reference curve with a value of α* = 0.0. In addition, a value of α* = 0.82 was reported for the MAS fiber of the jumping spider *Phidippus regius*, Salticidae, although this data was not obtained properly in the framework of the S3I, but during the preliminary work that led to the definition of the Initiative.

At this point it may be advisable to review a few aspects related to the definition and application of the α* parameter. To begin with, the possibility of classifying the tensile behaviour of MA silk with a single parameter may be considered as a consequence of the common design principles exhibited by these fibers (Perez-Rigueiro et al., 2021), even if spun by different species. In this regard, it is possible to identify three consecutive mechanisms that determine the mechanical behaviour of MA silk. Initially, the deformation of the material proceeds through the stretching of the hydrogen bonds established between the chains and corresponds to the elastic regime of the fibers. Subsequently, the hydrogen bonds get broken and the β-nanocrystals, formed by the piling up of the polyalanine runs, rotate and tend to increase their alignment with the macroscopic axis of the fiber. Lastly, the tensile properties of the material are controlled by the elatomeric behaviour of the protein chains, and by the formation of polyproline II nanocrystals from the aligned protein backbones (Perez-Rigueiro et al., 2021).

In this context, the different values of the α* parameter found in MA silks reflect quantitative differences in the extension of the second (rotation of the β-nanocrystals) and third (elastomeric deformation of the chains) micromechanisms, and in their contributions to the mechanical properties of fibers spun by different species. In particular, lower values of the α* parameter indicate a larger extension of these micromechanisms and, consequently, are correlated with higher values of strain at breaking and work to fracture. It should be highlighted at this point that the consideration of *A. aurantia* MAS to define the reference curve for calculating the α* parameter does not represent any constraint to the methodology, since the assignment of the value α* = 0.0 to this curve is purely conventional, and does not preclude the possibility of finding species whose MA silks exhibit negative values. These negative values would simply correspond to displacements of the true stress-true strain curves to the left along the true strain axis (X-axis). In spite of the conventional character of the assignment of the reference curve to the MAS spun by *A. aurantia*, it is observed in Fig. 3 how the lowest values of the α* parameter seem to be consistently found in representatives of the Araneoidea group. In this regard, it may be hypothesized whether this accumulation of low α* values may be related with the presence of MaSp2 proteins and their characteristic -GPG-motif among the constituent elements of MA silk in the spiders that belong to this group.

The proposal of the seminal hypotheses presented above indicate that the Spider Silk Standardization Initiative may be a useful tool to establish the relationship between phylogeny and/or ecology, and the tensile properties of the MAS fibers spun by different spider species. In turn, the usage of this systematic approach should contribute to clarify both the molecular basis that lead to the distinct properties of MA silks, and to identify the evolutionary pressures that modelled these properties

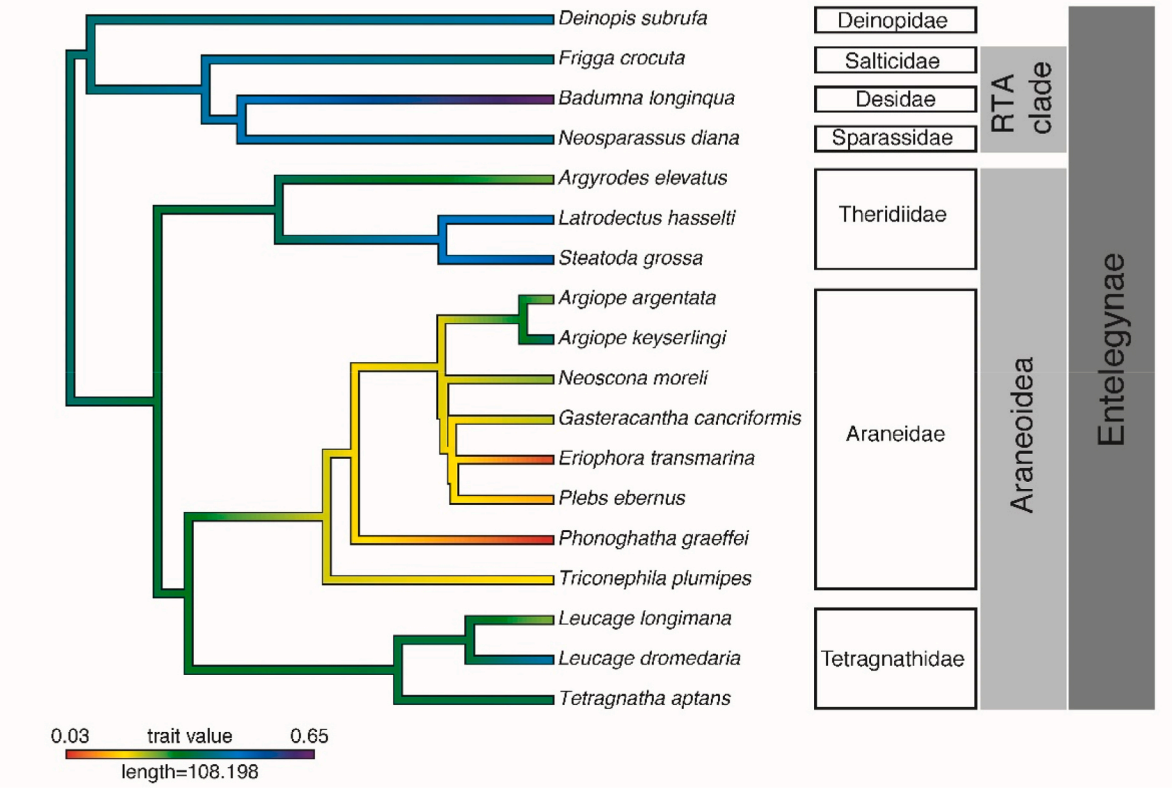

Fig. 3. Phylogenetic distribution of the values of the α* parameter across all the characterized species.

among different spider species.

4. Conclusions

The available values of the alignment parameter, α*, obtained in the framework of the Spider Silk Standardization Initiative (S3I; www.ctb.upm.es/core-facilities/) are significantly expanded in this work by adding the parameters measured from 11 Australian spider species. The values are comprised in the range between $\alpha^* = 0.03$ and $\alpha^* = 0.65$ and the combination of these new values with those previously included in the S3I allows testing the following hypotheses:

(1) When all species are considered with no other selection condition, the alignment parameter follows an approximately uniform distribution. It cannot be discarded, however, that the addition of new values of the α* parameter may lead to a refinement of this overall uniform distribution and establish the presence of some maxima or minima depending, for instance, on the phylogeny or ecology of the species and/or the typology of the webs built by the different species.
(2) In particular, the combination of the S3I analysis with the phylogenetic data indicates that the lowest values of the α* parameter are found in the Araneidae group, and tend to increase with the evolutionary distance of a given species to this group. This tendency, however, is not monotonous, with a significant number of outliers. For instance, two *Argiope* spiders present the largest values among the representatives of the Araneidae included in this work, despite the value of $\alpha^* = 0.0$ is established taken a species of this genus (*A. aurantia)* as Reference.

As indicated by the discussion above, the power of the S3I and other comparable approaches will depend on the availability of sufficient accurate data that, in turn, will allow undertaking rigorous analysis of the relationship of the measured tensile properties with the phylogeny and/or ecology of the spiders. These results are expected to have a profound influence in such varied areas as Materials Science, Evolutionary Biology and Biotechnology, since will represent a significant contribution to clarify some critical aspects of spider silk fibers. This additional knowledge may not only increase our fundamental understanding on the relationship between the properties of the material and the evolutionary pressures that modelled it, but also enhance our ability to design high performance and environmentally friendly fibers.

CRediT authorship contribution statement

Sean Blamires: Investigation. **Paloma Lozano-Picazo:** Investigation. **Augusto Luis Bruno:** Investigation. **Miquel Arnedo:** Investigation. **Yolanda Ruiz-León:** Investigation. **Daniel González-Nieto:** Formal analysis. **Francisco Javier Rojo:** Formal analysis. **Manuel Elices:** Supervision. **Gustavo Víctor Guinea:** Supervision. **José Pérez-Rigueiro:** Writing – original draft.

Declaration of competing interest

The authors declare that they have no known competing financial interests or personal relationships that could have appeared to influence the work reported in this paper.

Data availability

Data will be made available on request.

Acknowledgements

This study was partially funded by the Ministerio de Ciencia e Innovación (PID2020-116403RB-I00; MCIN/AEI/10.13039/501100011033) and by Comunidad de Madrid (Spain) through grant Tec4Bio-CM/P2018/NMT-4443. Additional funding was received from the Fondo Europeo de Desarrollo Regional (FEDER), as response of the EU to the COVID-19 pandemics through the COVITECH-CM project.

Appendix A. Supplementary data

Supplementary data to this article can be found online at https://doi.org/10.1016/j.jmbbm.2023.105729.

References

Anonymous, 2019. World Spider Catalog. Natural History Museum Bern. https://doi.org/10.24436/2.2019, Version 20.5.
Anton, A.M., Heidebrecht, A., Mahmood, N., Beiner, M., Scheibel, T., Kremer, F., 2017. Foundation of the outstanding toughness in biomimetic and natural spider silk. Biomacromolecules 18, 3954–3962.
Aparecido dos Santos-Pinto, J.R., Arcuri, H.A., Esteves, F.G., Palma, M.S., Lubec, G., 2018. Spider silk proteome provides insight into the structural characterization of Nephila clavipes flagelliform spidroin. Sci. Rep. 8, 14674.
Aparecido dos Santos-Pinto, J.R., Esteves, F.G., Sialana, F.J., Ferro, M., Smidak, R., Rares, L.C., Nussbaumer, T., Rattei, T., Bilban, M., Bacci Junior, M., et al., 2019. A proteotranscriptomic study of silk-producing glands from the orb-weaving spiders. Molecular Omics 15, 256–270.
Arakawa, K., Kono, N., Malay, A.D., Tateishi, A., Ifuku, N., Masunaga, H., Sato, R., Tsuchiya, K., Ohtoshi, R., Pedrazzoli, D., et al., 2022. 1000 Spider Silkomes: Linking Sequences to Silk Physical Properties. *Science advances* in press.
Asakura, T., Tasei, Y., Aoki, A., Nishimura, A., 2018. Mixture of rectangular and staggered packing arrangements of polyalanine region in spider dragline silk in dry and hydrated states as revealed by C-13 NMR and X-ray diffraction. Macromolecules 51, 1058–1068.
Benamu, M., Lacava, M., Garcia, L.F., Santana, M., Fang, J., Wang, X., Blamires, S.J., 2017. Nanostructural and mechanical property changes to spider silk as a consequence of insecticide exposure. Chemosphere 181, 241–249.
Blackledge, T.A., Hayashi, C.Y., 2006. Silken toolkits: biomechanics of silk fibers spun by the orb web spider Argiope argentata (Fabricius 1775). J. Exp. Biol. 209, 2452–2461.
Blackledge, T.A., Scharff, N., Coddington, J.A., Szuts, T., Wenzel, J.W., Hayashi, C.Y., Agnarsson, I., 2009. Reconstructing web evolution and spider diversification in the molecular era. Proc. Natl. Acad. Sci. U.S.A. 106, 5229–5234.
Blackledge, T.A., Pérez-Rigueiro, J., Plaza, G.R., Perea, B., Navarro, A., Guinea, G.V., Elices, M., 2012. Sequential origin in the high performance properties of orb spider dragline silk. Sci. Rep. 2, 782.
Blamires, S., 2022. Silk. Exploring Nature's Superfibre. XLibris Corporation.
Blamires, S.J., 2010. Plasticity in extended phenotypes: orb web architectural responses to variations in prey parameters. J. Exp. Biol. 213, 3207–3212.
Blamires, S.J., Blackledge, T.A., Tso, I.-., 2017a. Physicochemical property variation in spider silk: ecology, evolution, and synthetic production. Annu. Rev. Entomol. *62*, 443.
Blamires, S.J., Hasemore, M., Martens, P.J., Kasumovic, M.M., 2017b. Diet-induced covariation between architectural and physicochemical plasticity in an extended phenotype. J. Exp. Biol. 220, 876–884.
Blamires, S.J., Nobbs, M., Martens, P.J., Tso, I.-., Chuang, W., Chang, C., Sheu, H., 2018. Multiscale mechanisms of nutritionally induced property variation in spider silks. PLoS One 13, e0192005.
Boutry, C., Blackledge, T.A., 2010. Evolution of supercontraction in spider silk: structure-function relationship from tarantulas to orb-weavers. J. Exp. Biol. 213, 3505–3514.
Dunaway, D.L., Thiel, B.L., Viney, C., 1995. Tensile mechanical property evaluation of natural and epoxide-treated silk fibers. J. Appl. Polym. Sci. 58, 675–683.
Elices, M., Perez-Rigueiro, J., Plaza, G., Guinea, G.V., 2004. Recovery in spider silk fibers. J. Appl. Polym. Sci. 92, 3537–3541.
Garrote, J., Ruiz, V., Troncoso, O.P., Torres, F.G., Arnedo, M., Elices, M., Guinea, G.V., Perez-Rigueiro, J., 2020. Application of the Spider Silk Standardization Initiative ((SI)-I-3) methodology to the characterization of major ampullate gland silk fibers spun by spiders from Pantanos de Villa wetlands (Lima, Peru). J. Mech. Behav. Biomed. Mater. 111, 104023.
Gosline, J.M., Denny, M.W., Demont, M.E., 1984. Spider silk as rubber. Nature 309, 551–552.
Guinea, G.V., Perez-Rigueiro, J., Plaza, G.R., Elices, M., 2006. Volume constancy during stretching of spider silk. Biomacromolecules 7, 2173–2177.
Hansell, M., 2007. Built by Animals. Oxford University Press, Oxford.
Heim, M., Keerl, D., Scheibel, T., 2009. Spider silk: from soluble protein to extraordinary fiber. Angew. Chem., Int. Ed. Engl. 48, 3584–3596.
Madsen, B., Shao, Z.Z., Vollrath, F., 1999. Variability in the mechanical properties of spider silks on three levels: interspecific, intraspecific and intraindividual. Int. J. Biol. Macromol. 24, 301–306.
Madurga, R., Plaza, G.R., Blackledge, T.A., Guinea, G.V., Elices, M., Perez-Rigueiro, J., 2016. Material properties of evolutionary diverse spider silks described by variation in a single structural parameter. Sci. Rep. 6, 18991.
Perez-Rigueiro, J., Elices, M., Guinea, G.V., 2003. Controlled supercontraction tailors the tensile behaviour of spider silk. Polymer 44, 3733–3736.

Perez-Rigueiro, J., Viney, C., Llorca, J., Elices, M., 1998. Silkworm silk as an engineering material. J. Appl. Polym. Sci. 70, 2439–2447.
Perez-Rigueiro, J., Elices, M., Plaza, G.R., Guinea, G.V., 2021. Basic Principles in the Design of Spider Silk Fibers, vol. 26.
Perez-Riguero, J., Elices, M., Llorca, J., Viney, C., 2001. Tensile properties of Argiope trifasciata drag line silk obtained from the spider's web. J. Appl. Polym. Sci. 82, 2245–2251.
Riekel, C., Branden, C., Craig, C., Ferrero, C., Heidelbach, F., Muller, M., 1999. Aspects of X-ray diffraction on single spider fibers. Int. J. Biol. Macromol. 24, 179–186.
Rudall, K.M., Kenchington, W., 1971. Arthropod silks the problem of fibrous proteins in animal tissues. Annu. Rev. Entomol. 73–96.
Selden, P.A., Shear, W.A., Sutton, M.D., 2008. Fossil evidence for the origin of spider spinnerets, and a proposed arachnid order. Proc. Natl. Acad. Sci. U.S.A. 105, 20781–20785.
Swanson, B.O., Blackledge, T.A., Summers, A.P., Hayashi, C.Y., 2006. Spider dragline silk: correlated and mosaic evolution in high-performance biological materials. Evolution 60, 2539–2551.
Viera, C., Garcia, L.F., Lacava, M., Fang, J., Wang, X., Kasumovic, M.M., Blamires, S.J., 2019. Silk physico-chemical variability and mechanical robustness facilitates intercontinental invisibility of a spider. Sci. Rep. 9, 13273.
Vollrath, F., 1994. General-properties of some spider silks. Silk Polymers 544, 17–28.
Work, R.W., 1977. Dimensions, birefringences, and force-elongation behavior of major and minor ampullate silk fibers from orb-web-spinning spiders - effects of wetting on these properties. Textil. Res. J. 47, 650–662.